

# The dual role of shear in large-scale dynamos

A. Brandenburg\*

NORDITA, Roslagstullsbacken 23, SE-10691 Stockholm, Sweden

Received 2008 Jun 2, accepted 2008 Jul 18

Published online 2008 Aug 30

**Key words** magnetic fields – magnetohydrodynamics (MHD)

The role of shear in alleviating catastrophic quenching by shedding small-scale magnetic helicity through fluxes along contours of constant shear is discussed. The level of quenching of the dynamo effect depends on the quenched value of the turbulent magnetic diffusivity. Earlier estimates that might have suffered from the force-free degeneracy of Beltrami fields are now confirmed for shear flows where this degeneracy is lifted. For a dynamo that is saturated near equipartition field strength those estimates result in a 5-fold decrease of the magnetic diffusivity as the magnetic Reynolds number based on the wavenumber of the energy-carrying eddies is increased from 2 to 600. Finally, the role of shear in driving turbulence and large-scale fields by the magneto-rotational instability is emphasized. New simulations are presented and the  $3\pi/4$  phase shift between poloidal and toroidal fields is confirmed. It is suggested that this phase shift might be a useful diagnostic tool in identifying mean-field dynamo action in simulations and to distinguish this from other scenarios invoking magnetic buoyancy as a means to explain migration away from the midplane.

© 2008 WILEY-VCH Verlag GmbH & Co. KGaA, Weinheim

## 1 Introduction

Shear clearly plays an important role in amplifying toroidal fields from poloidal, but that is not all. Shear also plays a role in “unquenching” any dynamo effect that may play a role in producing poloidal field from toroidal, thus closing the dynamo loop. A prime example of such a dynamo effect is the  $\alpha$  effect, but other possible known effects may include the shear-current effect and the incoherent alpha-shear effect. The “unquenching” of dynamo effects, as well as the dynamo effects themselves, require more detailed considerations of the results available so far. This is the principal goal of this paper.

The term “unquenching” in connection with the  $\alpha$  effect may appear somewhat unusual, but this choice of words must be seen in contrast to the possibility of catastrophic  $\alpha$  quenching. Here, “catastrophic” indicates that the quenching by the mean magnetic field,  $\overline{\mathbf{B}}$ , becomes more extreme as the magnetic Reynolds number,  $R_m$ , increases. Traditionally, such quenching is represented by the simplistic formula (Vainshtein & Cattaneo 1992)

$$\alpha(\overline{\mathbf{B}}) = \frac{\alpha_0}{1 + R_m \overline{\mathbf{B}}^2 / B_{\text{eq}}^2}, \quad (1)$$

where  $B_{\text{eq}} = \langle \mu_0 \rho \mathbf{u}^2 \rangle^{1/2}$  is the equipartition field strength with respect to the kinetic energy density,  $\mathbf{u}$  is the small-scale turbulent velocity,  $\rho$  is the density,  $\mu_0$  is the vacuum permeability,  $R_m = u_{\text{rms}} / \eta k_f$  is the magnetic Reynolds number,  $\eta$  is the magnetic diffusivity,  $k_f$  is the wavenumber of the energy-carrying scale, and angular brackets denote volume averaging. However, Eq. (1) is really only valid

under special circumstances that are quite uninteresting for dynamo action: infinite wavelength of the magnetic field, complete stationarity, and no possibility of magnetic helicity fluxes. The latter possibility is now believed to be the most important one for astrophysical dynamos, as was first suggested by Blackman & Field (2000). Any one of these three caveats alleviates the severity of catastrophic quenching, because they all lead to “extra terms” that enter in the numerator of Eq. (1) with an  $R_m$  factor in front, i.e.

$$\alpha(\overline{\mathbf{B}}) = \frac{\alpha_0 + R_m \times \text{“extra effects”}}{1 + R_m \overline{\mathbf{B}}^2 / B_{\text{eq}}^2}, \quad (2)$$

where we have assumed that the kinematic  $\alpha$  value,  $\alpha_0$ , remains independent of time. In its essence, this equation with extra effects included goes back to the early work of Kleeorin & Ruzmaikin (1982), and later Kleeorin et al. (1995, 2000), and has been discussed in connection with alleviating catastrophic  $\alpha$  quenching by Blackman & Brandenburg (2002) and Brandenburg & Subramanian (2005a). A more complete quenching formula with extra effects included takes the form

$$\alpha = \frac{\alpha_0 + R_m \left( \eta_t \frac{\mu_0 \overline{\mathbf{J}} \cdot \overline{\mathbf{B}}}{B_{\text{eq}}^2} - \frac{\nabla \cdot \overline{\mathcal{F}}_c}{2k_f^2 B_{\text{eq}}^2} - \frac{\partial \alpha / \partial t}{2\eta_t k_f^2} \right)}{1 + R_m \overline{\mathbf{B}}^2 / B_{\text{eq}}^2}. \quad (3)$$

Let us now discuss separately all three terms in the parenthesis of the numerator of Eq. (3).

(i) The effect of the  $\overline{\mathbf{J}} \cdot \overline{\mathbf{B}}$  term is clearly seen when considering the saturation of homogeneous dynamos in a periodic domain. In that case this formula gives

$$\alpha(\overline{\mathbf{B}}) \rightarrow \eta_t \mu_0 \overline{\mathbf{J}} \cdot \overline{\mathbf{B}} / \overline{\mathbf{B}}^2 \quad (\text{for } R_m \rightarrow \infty), \quad (4)$$

so there is nothing catastrophic about this formula, unless  $\eta_t$  itself is catastrophically quenched. Of course, if mean

\* Corresponding author: brandenb@nordita.org

fields are defined as full volume averages,  $\overline{\mathbf{B}}$  becomes completely uniform, so  $\mu_0 \overline{\mathbf{J}} = \nabla \times \overline{\mathbf{B}} = 0$ . This is the case in numerical experiments by Cattaneo & Hughes (1996). The other case with a finite  $\overline{\mathbf{J}} \cdot \overline{\mathbf{B}}$  term was seen in the simulations of Brandenburg (2001), where not only a large-scale magnetic field was found to saturate at super-equipartition values, but also the  $\alpha$  and  $\eta_t$  effects were found to be only mildly quenched.

(ii) The  $\partial/\partial t$  term in Eq. (3) is important to explain the absence of an otherwise premature onset of quenching at resistively low field strengths where  $\overline{\mathbf{B}}^2/B_{\text{eq}}^2 \approx R_m^{-1}$ . This is also confirmed by controlled numerical experiments where the initial field was a weak Beltrami field (Brandenburg et al. 2003).

(iii) Finally, the effect of magnetic helicity fluxes was first seen in simulations with imposed fields by Brandenburg & Sandin (2004), and then later in dynamo simulations (Brandenburg 2005a), which brings us to the main topic of this paper. As was already seen in earlier simulations without shear, just allowing for open boundary conditions alone does not help to produce a finite magnetic helicity flux in Eq. (3) and hence does not alleviate catastrophic  $\alpha$  quenching (Brandenburg & Dobler 2001). However, Vishniac & Cho (2001) showed that in the presence of differential rotation a magnetic helicity flux can be generated and that it flows along the rotation axis. More detailed work of Subramanian & Brandenburg (2004, 2006) and Brandenburg & Subramanian (2005b) resulted in a simple formula for this particular contribution to the flux:

$$\overline{\mathcal{F}}_C = C_{VC}(\overline{\mathbf{S}}\overline{\mathbf{B}}) \times \overline{\mathbf{B}}, \quad (5)$$

where  $\overline{\mathbf{S}}_{ij} = \frac{1}{2}(\overline{U}_{i,j} + \overline{U}_{j,i})$  is the rate of strain matrix of the mean flow, and  $C_{VC}$  is a dimensionless number of order unity. This flux is along contours of constant shear, as was demonstrated by Brandenburg et al. (2005); see also Fig. 1.

The sign of the magnetic helicity flux is negative in the Northern hemisphere, so vectors of positive magnetic helicity flux point away from the surface in the Northern hemisphere, then through the equator and into the Southern hemisphere.

## 2 Quantitative considerations

Simulations of Brandenburg & Sandin (2004) indicate that the magnitude of the Vishniac-Cho flux might be on the order of  $10^{46} \text{ Mx}^{24}/\text{cycle}$ , if applied to the Sun. In units of  $\overline{\mathcal{F}}_0 \equiv u_{\text{rms}} k_f B_0^2$  the nondimensional flux was estimated to be about  $30/\frac{1}{2}\text{Sh}$ , where

$$\text{Sh} \equiv S/u_{\text{rms}} k_f \quad (6)$$

is the nondimensional shear parameter and  $S$  is the shear rate. The corresponding  $C_{VC}$  parameter would then be  $\gg 1$ . This result appears in conflict with the expectation that  $C_{VC}$  should be of order unity (Subramanian & Brandenburg 2004; Brandenburg & Subramanian 2005b). It would therefore be important to return to this issue using a simpler

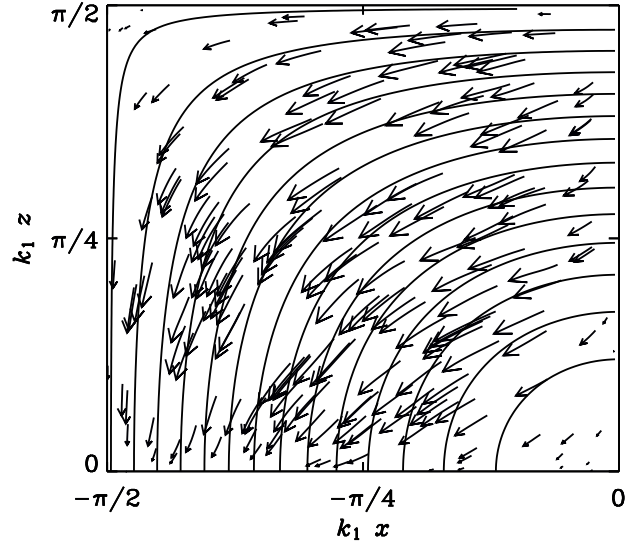


**Fig. 1** Vectors of  $\overline{\mathcal{F}}_C$  together with contours of  $\overline{U}_y$  which also coincide with the streamlines of the mean vorticity field  $\overline{\mathbf{W}}$ . Note the close agreement between  $\overline{\mathcal{F}}_C$  vectors and  $\overline{\mathbf{W}}$  contours. The orientation of the vectors indicates that negative current helicity leaves the system at the outer surface ( $x = 0$ ). Adapted from Brandenburg et al. (2005).

one-dimensional shear profile together with open boundary conditions.

A more conclusive indication for the operation of helicity fluxes is the demonstration of a successful dynamo simulation; see, e.g., Brandenburg (2005a), where it was also demonstrated that with closed perfect conductor boundary conditions the dynamo was not successful in producing large-scale fields (at least not during the course of the present simulation). In Fig. 2 we plot the ratio of the energy contained in the large-scale field to the total magnetic energy. We see clearly that large-scale dynamo action is only possible with open boundary conditions. By open we mean here the vertical field condition that is commonly used in simulations of magneto-convection (Hurlburt & Toomre 1988). Such boundary conditions do permit a finite magnetic helicity flux, but they do not allow Poynting flux to pass through the boundaries. It is at present unclear whether the absence of a Poynting flux is a serious short-coming or not.

Another remarkable result found in the work of Brandenburg (2005a) is that large-scale magnetic fields can be found even without kinetic helicity and hence without  $\alpha$  effect. An obvious possibility might be that this is caused by the shear-current effect of Rogachevskii & Kleeorin (2003, 2004). However, in the case of a simpler geometry where the contours of constant shear are purely vertical, which is relevant for accretion discs, for example, no direct support for the existence of this effect has been found (Brandenburg 2005b; Brandenburg et al. 2008a). This is also consistent with earlier analytic results of Rüdiger & Kitchatinov

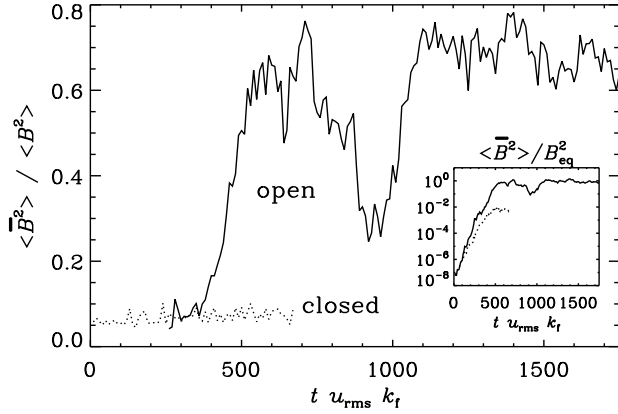


**Fig. 2** Evolution of the ratio of the energies contained in the large-scale field to the total magnetic energy for open and closed boundaries. Note that large-scale dynamo action is only possible with open (vertical field) boundary conditions. Adapted from Brandenburg (2005a).

(2006) and Rädler & Stepanov (2006) using the second order correlation approximation (SOCA). In essence, a shear-current effect would be described by a mean-field equation with an anisotropic magnetic diffusion tensor,  $\eta_{ij}$ . We write the governing equation here for the magnetic vector potential,

$$\frac{D\bar{A}_i}{Dt} = -\bar{A}_j \bar{U}_{j,i} - \mu_0 \eta_{ij} \bar{J}_j - \mu_0 \eta \bar{J}_i, \quad (7)$$

where  $\bar{\mathbf{J}} = -\nabla^2 \bar{\mathbf{A}}$ , and one-dimensional averages have been employed, i.e.  $\bar{\mathbf{J}} = \bar{\mathbf{J}}(z, t)$  in the present case, and  $\bar{\mathbf{U}} = (0, Sx, 0)$ . In the case of vertical contours of the mean shear, we have  $\bar{U}_{2,1} = S$  and all other components vanish. Here, the cross-stream direction is  $i = x$  or 1, and the streamwise direction is  $i = y$  or 2.

In order to have a closed dynamo loop, one would then need to have a finite  $\eta_{21}$  component with the same sign as that of  $S$ . According to SOCA calculations and simulations this is however not the case. In Fig. 3 we show the resulting values of  $\eta_{21}$  for such a linear shear flow, as obtained using the testfield method.

Here we have used  $S < 0$ , so we are looking for negative values of  $\eta_{21}$  for an operational shear-current effect. In all cases we find  $\eta_{21} > 0$ , except for large values of  $R_m$  when  $P_m = 20$ . However, the error bars are large. There is perhaps the possibility that the sign of  $\eta_{21}$  may change under other circumstances, e.g. for the more complicated shear profile shown in Fig. 1. Yet another possibility is that in the presence of helicity the sign may change. Some evidence to this effect has been provided by Mitra et al. (2008). It turns out that in nonhelical shear flow turbulence,  $\eta_{21}$  can become negative in the saturated state with helicity. However, given that there is still an  $\alpha$  effect, the relevance of the shear-current effect is less obvious in these simulations.

Obviously, with helicity there is also an  $\alpha$  effect, so the shear-current effect would not be the sole cause of large-scale dynamo action. This leaves us with the question what

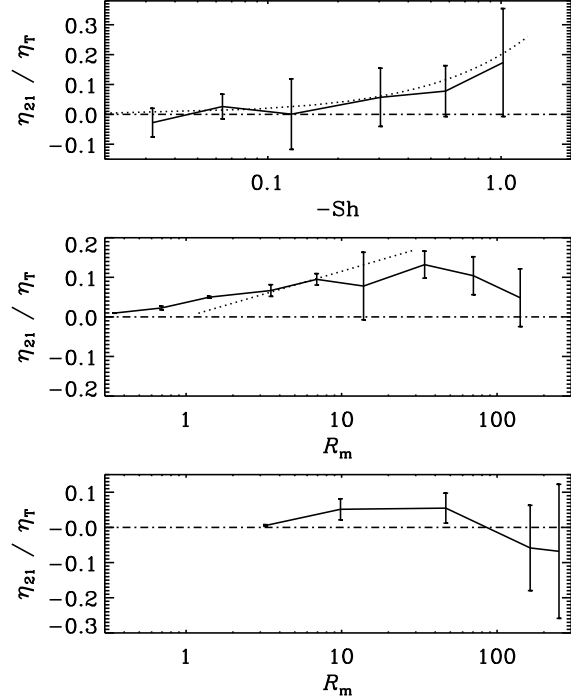


**Fig. 3** Dependence of  $\eta_{21}$ , normalized by the total (turbulent and microscopic) magnetic diffusivity on shear parameter (upper panel) and on magnetic Reynolds number for  $Re = 1.4$  (middle panel) and for a fixed magnetic Prandtl number,  $P_m = 20$  (lower panel). Adapted from Brandenburg et al. (2008a).

causes large-scale magnetic field generation in non-helical turbulence with shear? In addition to the simulations of Brandenburg (2005a), discussed above, there are also simulations of Yousef et al. (2008), where a large-scale magnetic field is generated. They find a growth rate that is proportional to the shear rate  $S$ . The authors argue that such a result would not be consistent with the shear-current effect, because the growth rate would then be proportional to the product of  $S$  and  $\eta_{21}$ , where  $\eta_{21}$  itself would be proportional to  $S$ .

The alternative proposal by Brandenburg et al. (2008a) is that an incoherent  $\alpha$ -shear or  $\alpha\Omega$  dynamo is at work. The occurrence of an incoherent  $\alpha$ -shear dynamo (cf. Vishniac & Brandenburg 1997; Proctor 2007; Kleeorin & Rogachevskii 2008) was quantified by estimating the rms values of the fluctuations of all components of  $\alpha_{ij}$  and  $\eta_{ij}$ . Figure 4 shows how these rms values vary with increasing values of  $R_m$ . We recall that the average of all components of  $\alpha_{ij}$  is zero, so there is no regular  $\alpha$  effect. The onset of incoherent dynamo action depends on the value of the dynamo number

$$D_{\alpha S}^{\text{incoh}} = \alpha_{\text{rms}} S / \eta_T k_1^3, \quad (8)$$

where  $\alpha_{\text{rms}}$  is the rms value of the streamwise component  $\alpha_{22}$  (but all components are found to have the same rms value),  $\eta_T = \eta_T + \eta$  is the sum of turbulent and micro-

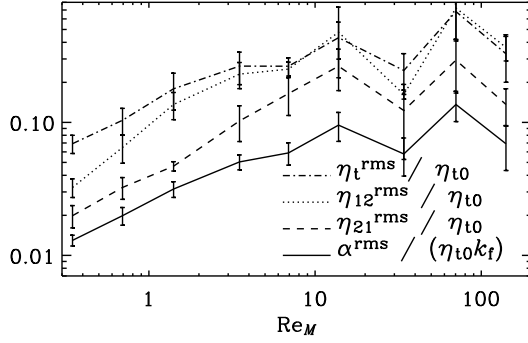


**Fig. 4** Dependences of the rms values of the temporal fluctuations  $\alpha_{\text{rms}}$  (normalized by  $\eta_{t0}k_f$ ),  $\eta_t^{\text{rms}}$ ,  $\eta_{21}^{\text{rms}}$ , and  $\eta_{12}^{\text{rms}}$  (normalized by  $\eta_{t0}$ ), on  $R_m$  for  $\text{Re} = 1.4$  and  $\text{Sh} = -0.6$ . Adapted from Brandenburg et al. (2008a).

scopic magnetic diffusivity, and  $k_1 = 2\pi/L$  is the lowest wavenumber in the  $z$  direction of the box.

The simulations of Brandenburg et al. (2008a) give fluctuations of  $\alpha_{\text{rms}}$  that correspond to  $D_{\alpha S}^{\text{incoh}} \approx 4$ . This is to be compared with the marginal value of  $\approx 2.3$  obtained numerically using a single-mode approximation. There is in principle also the incoherent shear-current effect, based on the random occurrence of values of  $\eta_{21}$  with suitable sign. However, the effect is found to be subdominant compared with the dynamo number of the incoherent  $\alpha$ -shear dynamo. Yet another possibility for generating large-scale magnetic fields in the presence of shear is given by additive noise in the electromotive force due to small-scale dynamo action (Blackman 1998). However, in Yousef et al. (2008) no small-scale dynamo was excited, so this type of noise would not explain the field seen in their simulation.

In all cases one would expect random reversals of the toroidal magnetic field on a turbulent diffusion time scale. However, simulations usually give longer time scales, which may be explained by a tendency to conserve magnetic helicity. Indeed, using magnetic helicity conservation, Brandenburg et al. (2008a) found that in a closed domain the reversal time increases with  $R_m$  to the  $1/2$  power. The mean reversal time might therefore well be much larger than a turbulent diffusion time.

### 3 Shear in helical turbulent dynamos

Let us now look at the effects of shear in simulations where kinetic helicity and thus an  $\alpha$  effect are present. In these cases there is the possibility of oscillatory solutions with frequency  $\omega_{\text{cyc}}$  and propagating dynamo waves of wavenumber  $k$  and wave speed  $c = \omega_{\text{cyc}}/k$ . The sense of propagation is determined by the sign of the product  $\alpha S$ . When shear is sufficiently strong ( $|S/\alpha k| \gg 1$  or, equivalently,  $|\text{Sh}| \gg \frac{1}{3}k_1/k_f$  for fully helical turbulence with  $\alpha \approx \frac{1}{3}u_{\text{rms}}$ ), the magnitude of the oscillation frequency is given by  $(\alpha k S/2)^{1/2}$ , but in the marginal state this must be balanced by the diffusion rate  $\eta_T k^2$ . As was stressed

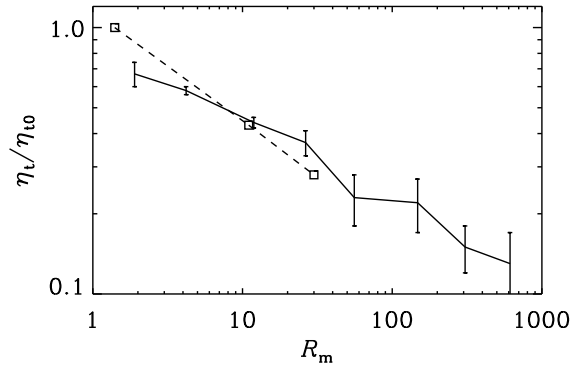


**Fig. 5**  $R_m$  dependence of  $\eta_t$  in the dynamo-saturated state as measured by the testfield method (solid line; Brandenburg et al. 2008b), and estimated for oscillatory  $\alpha\Omega$  dynamos in a shearing box (dashed line; Käpylä & Brandenburg, in preparation).

by Blackman & Brandenburg (2002), this provides therefore a robust tool for determining empirically the quenched value of  $\eta_T = \eta_t + \eta$ . However, it has been rather hard to reach large enough values of the ratio  $\eta_t/\eta$  (which is also a proxy of  $R_m$ ) to make conclusive statements about the  $R_m$ -dependence of  $\eta_t$ . Indeed, the values obtained so far (Fig. 5) confirm recent results of Brandenburg et al. (2008b), where a measure of  $\eta_t$  has been obtained using the testfield method applied to the nonlinear state for  $R_m$  ranging between 2 and 600. Unfortunately, those results leave some ambiguity between the  $\alpha$  effect and the turbulent magnetic diffusivity, because of terms of the form  $(\overline{\mathbf{J}} \cdot \overline{\mathbf{B}})\overline{\mathbf{B}}$ , whose coefficients can be associated both with  $\alpha$  and with  $\eta_t$ .

## 4 MRI-driven turbulence

Interesting systems where the effects of shear play an absolutely vital role are seen in local simulations of accretion disc turbulence that is driven by the magneto-rotational instability (Hawley et al. 1995). When there is also stratification about the midplane, the Coriolis force produces an  $\alpha$  effect. Simulations of Brandenburg et al. (1995) give rise to large-scale dynamo action that turns out to be oscillatory with dynamo waves propagating away from the midplane. In Fig. 6 we show new simulations that are similar to those of Brandenburg et al. (1995), but with somewhat larger resolution and without using hyperviscosity. Only shock viscosity and shock resistivity are being used. Another difference is that these simulations also have a potential field boundary condition instead of the vertical field condition that was used in Brandenburg et al. (1995). Given the remarkable similarity with the earlier simulations, we must conclude that the different boundary conditions do not seem to have a major effect. The new simulations are similar in that they too show oscillations with a typical period of about

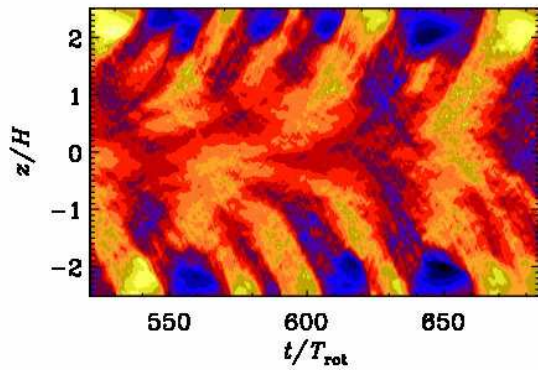


**Fig. 6** (online colour at: [www.an-journal.org](http://www.an-journal.org)) Space-time ( $z$ - $t$ ) diagram of  $\overline{B}_y(z, t)$  for a run where turbulence is driven by the magneto-rotational instability. The magnetic Reynolds number, based on the actual rms velocity and the pseudo wavenumber  $k_t = 2\pi/H$ , is about 120.

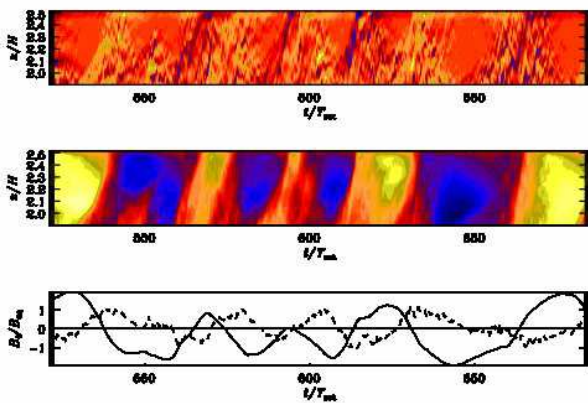


**Fig. 7** (online colour at: [www.an-journal.org](http://www.an-journal.org)) Mean poloidal and toroidal fields in a narrow slice near the upper disc plane as a function of  $t$  and  $z$ , together with the averages over the same slice showing the phase relation between the two. The solid line indicates  $\overline{B}_y/B_{\text{eq}}$  while the dotted line indicates  $\overline{B}_x/B_{\text{eq}}$ , scaled up by a factor of 20 to make it better visible.

30–50 orbits (the orbital time is defined as  $T_{\text{rot}} = 2\pi/\Omega$ ). However, the new simulations also show considerably more fluctuations with parity variations and, more importantly, a noticeable decoupling of behavior in the Northern and Southern disc planes. The parity varies therefore between more nearly symmetric (even) and more nearly antisymmetric (odd) parity.

## 5 Detecting mean-field dynamo action

A possible means of identifying  $\alpha\Omega$ -type dynamo action as the main course of oscillations seen in simulations we propose to determine the phase relation between poloidal and

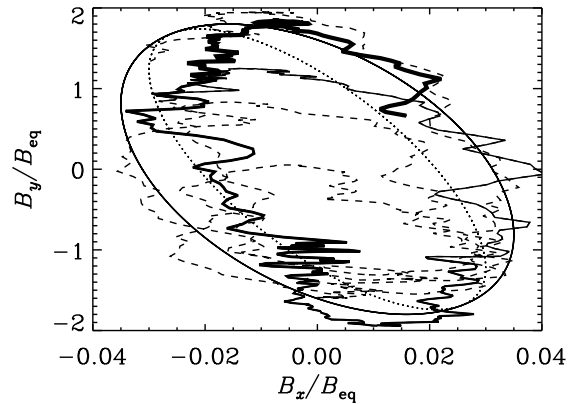


**Fig. 8** Phase plot of the averages of poloidal and toroidal fields over the same narrow slices as in Fig. 7. The first times are plotted as dashed lines, but the later times are solid with increasing thickness toward the end showing that a point on the curve moves forward in a clockwise direction. Overplotted are two ellipses showing  $B_{y0} \propto \cos(\omega t + \phi)$  versus  $B_{x0} \propto \cos \omega t$  with  $\phi = 0.65\pi$ ,  $B_{x0} = 0.035 B_{\text{eq}}$ , and  $B_{x0} = 1.8 B_{\text{eq}}$  (solid line) and  $\phi = 0.75\pi$ ,  $B_{x0} = 0.03 B_{\text{eq}}$ , and  $B_{x0} = 1.74 B_{\text{eq}}$  (dotted line).

toroidal fields. This used to be a standard tool in solar dynamo theory to infer the sense of radial differential rotation, but may also become an important tool in disc and other oscillatory dynamos. Mean-field theory predicts a phase shift by  $\frac{3}{4}\pi$ , which was confirmed by Brandenburg & Sokoloff (2002). Another alternative explanation for the migration away from the midplane would be magnetic buoyancy. This was discussed by Vishniac & Brandenburg (1997), who noted that the migration speed is only about 3% of the turbulent rms velocity. The idea of magnetic buoyancy playing a leading role was expressed again in connection with recent simulations of Blaes et al. (2008), where the outer disc surface is marked by a surface where the optical depth in a radiative transfer calculation was of order unity. However, no detailed proposal for the phase relation from the buoyancy effect has yet been made.

Brandenburg et al. (1995) found that the details of the large-scale magnetic field generation can be described by an  $\alpha$  effect that is negative in the Northern disc plane. Newer determinations of  $\alpha_{ij}$  and  $\eta_{ij}$  using the testfield method confirm this result also for the present simulations; see Fig. 9. Again, we have here access to all 4+4 components of the  $\alpha_{ij}$  and  $\eta_{ij}$  tensors. As in Brandenburg & Sokoloff (2002), who used a correlation method instead of the test-field method,  $\alpha_{yy}$  is negative in the upper midplane and has an extremum at  $z \approx \pm H$ . However,  $\alpha_{11} (\equiv \alpha_{xx})$  is positive in the upper disc plane.

In all cases we find that  $\eta_{11} \approx \eta_{22}$  and always positive, in contrast to earlier work using the correlation method. This function has a minimum in the midplane and grows

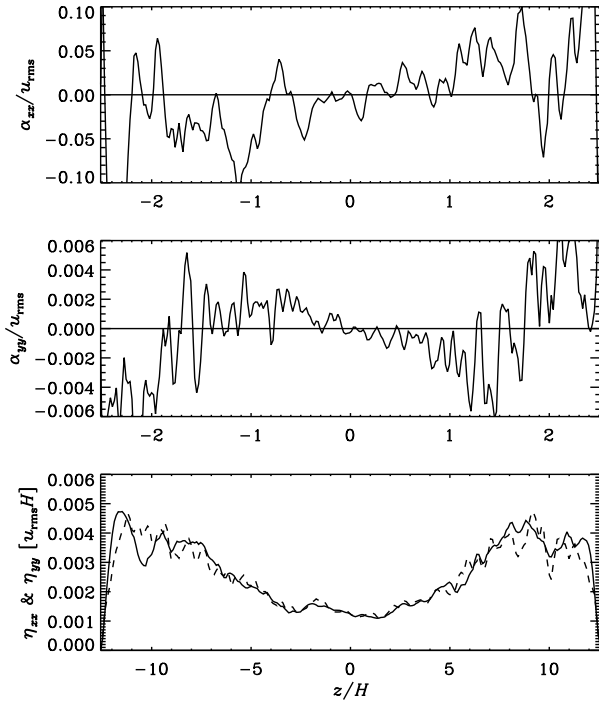


**Fig. 9** Vertical profiles of  $\alpha_{xx}$ ,  $\alpha_{yy}$  (first and second panel), both normalized by the turbulent rms velocity, as well as  $\eta_{xx}$  (solid line) and  $\eta_{yy}$  (dashed line) for an MRI disc simulations.

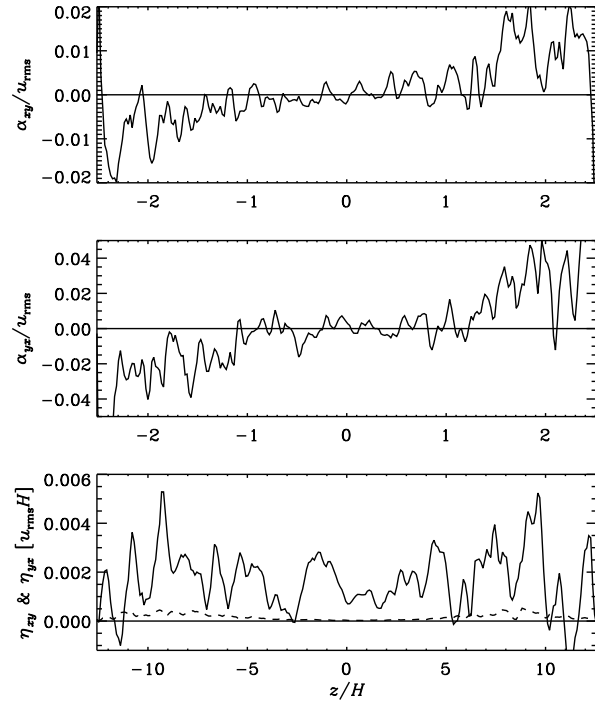


**Fig. 10** Vertical profiles of  $\alpha_{xy}$ ,  $\alpha_{yx}$  (first and second panel), both normalized by the turbulent rms velocity, as well as  $\eta_{xy}$  (solid line) and  $\eta_{yx}$  (dashed line) for an MRI disc simulations.

away from the midplane by a factor of about 4. The off-diagonal components of  $\alpha_{ij}$  and  $\eta_{ij}$  are shown in Fig. 10.

It turns out that, like  $\alpha_{xx}$  and  $\alpha_{yy}$ , also  $\alpha_{xy}$  and  $\alpha_{yx}$  are approximately antisymmetric about the midplane and positive in the upper disc plane. The off-diagonal components of  $\alpha_{ij}$  are normally interpreted in terms of turbulent pumping with an effective vertical velocity  $\gamma = \frac{1}{2}(\alpha_{yx} - \alpha_{xy})$ . However, since  $\alpha_{yx}$  and  $\alpha_{xy}$  have the same sign, there is some cancelation. Nevertheless, since  $\alpha_{yx}$  is larger than  $\alpha_{xy}$ , there is net transport away from the midplane. This concerns predominantly the toroidal field component,  $\overline{B}_y$ , while the poloidal component,  $\overline{B}_x$ , is transported predominantly toward the midplane. Such differential pumping of poloidal and toroidal fields was first discussed by Kitchatinov (1991) and later confirmed in simulations by Ossendrijver et al. (2002).

The off-diagonal components of  $\eta_{ij}$  are symmetric about the midplane and both are mainly positive. The  $\eta_{yx}$  component is important for the shear-current effect, but it is found to have the wrong sign for this effect to operate in our simulations; see also Sect. 2.

## 6 Dynamos in shearing convection

Large-scale dynamo action of significant amplitude has been seen in global simulations of the geodynamo (Glatzmaier & Roberts 1995). However, simulations in Cartesian

boxes have not yet shown such behavior. A recent example is that by Tobias et al. (2008) where strong shear was present. However, the absence of large-scale fields of significant magnitude may be related to the orientation of shear. In their case those contours are horizontal, so the Vishniac-Cho flux, that goes along those contours, would not be able to escape the horizontally periodic domain. If it is true that large-scale dynamo action only works efficiently if excess small-scale magnetic helicity is expelled through the boundaries, then it would be plausible that shear may not help the dynamo in all cases. More recent convection simulations by Käpylä et al. (2008) do show large-scale magnetic field in the presence of shear. They have contours of constant shear that do cross the boundaries. In fact, their shear is just like that in the accretion disc simulations discussed earlier.

## 7 Discussion

In this paper we have illustrated the important dual role played by shear: helping to produce strong toroidal field and helping to unquench the  $\alpha$  effect. We have tried to make the case that successful large-scale dynamos must have an opportunity to shed small-scale magnetic helicity through the boundaries. This is what the Sun does (e.g., Démoulin et al. 2002), and this is also what many simulations can do, although the degree of realism to which simulations can do this varies. So far, there is no simulation that goes all the way to including at least a simplified way of modeling coro-

nal mass ejections as the final stage in shedding small-scale magnetic helicity. This should obviously be tried in the near future using simulations in spherical shell segments, possibly with an additional outer layer where wind acceleration can occur (Brandenburg et al. 2007).

In this connection it might be helpful to explain the special meaning of “small scale” in connection with large-scale dynamos. In solar physics, one is used to associating active regions with large scales, while small scales would often refer to the resolution limit of 100 km or less. Obviously, in connection with the solar cycle, relevant time and length scales would be on the order of years and several hundred megameters, respectively – well encompassing the duration and size of active regions. In the present work we have used averages that do not a priori separate between large and small scales. By assuming an average over one or two coordinate directions (e.g. an azimuthal average for global simulations of the Sun, or horizontal averages in local box simulations), there could still be residual fluctuations on short time and small length scales, but they should go away with increasing system size in the azimuthal or horizontal directions like one over the square root of the number of eddies that are being averaged over. Exactly this fact is behind the operation of the incoherent  $\alpha$ -shear dynamo discussed at the end of Sect. 2. Clearly a finite horizontal extent is not only a numerical restriction of local boxes. Indeed, a finite azimuthal extent is bare reality even for the Sun. This point has been made by Hoyng (1993) in order to explain limits to the phase and amplitude stability of the solar cycle, but this very mechanism could even suffice to drive a dynamo in shearing systems where there is no  $\alpha$  effect present. It should be emphasized that the incoherent  $\alpha$  effect as such is independent of shear, but it is able to produce coherent large-scale fields only in the presence of shear. Obviously, more work is needed to sharpen the analytical and numerical tools to understand such systems better. Finally, let us emphasize that incoherent  $\alpha$ -effect dynamos too have a non-linear stage that is controlled by magnetic helicity at some level. In Brandenburg et al. (2008a) we only used a very simplistic one-mode truncation to make this point, but the whole dynamical quenching formalism applies otherwise just as well.

*Acknowledgements.* I thank Eric G. Blackman for comments on this paper and the organizers of the KITP program on dynamo theory for providing a stimulating atmosphere during its programs on dynamo theory. This research was supported in part by the National Science Foundation under grant PHY05-51164. Computational resources were made available by the Swedish National Allocations Committee at the National Supercomputer Centre in Linköping.

## References

- Blackman, E.G.: 1998, ApJ 496, L17  
 Blackman, E.G., Brandenburg, A.: 2002, ApJ 579, 359  
 Blackman, E.G., Field, G.B.: 2000, ApJ 534, 984  
 Blaes, O.M.: 2008, private communication

- Brandenburg, A.: 2001, ApJ 550, 824  
 Brandenburg, A.: 2005a, ApJ 625, 539  
 Brandenburg, A.: 2005b, AN 326, 787  
 Brandenburg, A., Dobler, W.: 2001, A&A 369, 329

- Brandenburg, A., Sokoloff, D.: 2002, *GAJFD* 96, 319
- Brandenburg, A., Sandin, C.: 2004, *A&A* 427, 13
- Brandenburg, A., Subramanian, K.: 2005a, *PhR* 417, 1
- Brandenburg, A., Subramanian, K.: 2005b, *AN* 326, 400
- Brandenburg, A., Nordlund, Å., Stein, R. F., Torkelsson, U.: 1995, *ApJ* 446, 741
- Brandenburg, A., Haugen, N.E.L., Dobler, W.: 2003, in: R. Erdélyi et al., *Turbulence, Waves, and Instabilities in the Solar Plasma*, p. 33
- Brandenburg, A., Haugen, N.E.L., Käpylä, P.J., Sandin, C.: 2005, *AN* 326, 174
- Brandenburg, A., Käpylä, P. J., Mitra, D., Moss, D., Tavakol, R.: 2007, *AN* 328, 1118
- Brandenburg, A., Rädler, K.-H., Rheinhardt, M., Käpylä, P.J.: 2008a, *ApJ* 676, 740
- Brandenburg, A., Rädler, K.-H., Rheinhardt, M., Subramanian, K.: 2008b, *ApJ*, arXiv 0805.1287
- Cattaneo, F., Hughes, D.W.: 1996, *Phys Rev E* 54, R4532
- Démoulin, P., Mandrini, C.H., van Driel-Gesztelyi, L., Thompson, B.J., Plunkett, S., Kovári, Z., Aulanier, G., Young, A.: 2002, *ApJ* 382, 650
- Glatzmaier, G.A., Roberts, P.H.: 1995, *Nature* 377, 203
- Hawley, J.F., Gammie, C.F., Balbus, S.A.: 1995, *ApJ* 440, 742
- Hoyng, P.: 1993, *A&A* 272, 321
- Hurlburt, N.E., Toomre, J.: 1988, *ApJ* 327, 920
- Käpylä, P.J., Korpi, M.J., Brandenburg, A.: 2008, *A&A*, arXiv 0806.0375
- Kitchatinov, L.L.: 1991, *A&A* 243, 483
- Kleeorin, N.I., Ruzmaikin, A.A.: 1982, *Magnetohydrodynamics* 18, 116
- Kleeorin, N., Rogachevskii, I.: 2008, *Phys Rev E* 77, 036307
- Kleeorin, N., Rogachevskii, I., Ruzmaikin, A.: 1995, *A&A* 297, 159
- Kleeorin, N., Moss, D., Rogachevskii, I., Sokoloff, D.: 2000, *A&A* 361, L5
- Mitra, D., Käpylä, P.J., Tavakol, R., Brandenburg, A.: 2008, *A&A*, arXiv 0806.1608
- Ossendrijver, M., Stix, M., Brandenburg, A., Rüdiger, G.: 2002, *A&A* 394, 735
- Proctor, M.R.E.: 2007, *MNRAS* 382, L39
- Rädler, K.-H., Stepanov, R.: 2006, *Phys Rev E* 73, 056311
- Rogachevskii, I., Kleeorin, N.: 2003, *Phys Rev E* 68, 036301
- Rogachevskii, I., Kleeorin, N.: 2004, *Phys Rev E* 70, 046310
- Rüdiger, G., Kitchatinov, L.L.: 2006, *AN* 327, 298
- Subramanian, K., Brandenburg, A.: 2004, *Phys Rev Lett* 93, 205001
- Subramanian, K., Brandenburg, A.: 2006, *ApJ* 648, L71
- Tobias, S.M., Cattaneo, F., Brummell, N.H.: 2008, *ApJ* preprint, doi:10.1086/590422
- Vainshtein, S.I., Cattaneo, F.: 1992, *ApJ* 393, 165
- Vishniac, E.T., Brandenburg, A.: 1997, *ApJ* 475, 263
- Vishniac, E.T., Cho, J.: 2001, *ApJ* 550, 752
- Yousef, T.A., Heinemann, T., Schekochihin, A.A., Kleeorin, N., Rogachevskii, I., Iskakov, A.B., Cowley, S.C., McWilliams, J.C.: 2008, *Phys Rev Lett* 100, 184501